

https://doi.org/10.1070/QEL17310

Accuracy of the duration estimates of ultrashort laser pulses using a single-shot second-order intensity autocorrelator

I.V. Kuzmin, S.Yu. Mironov, E.A. Khazanov

Abstract. **The accuracy of estimating the duration of single-cycle laser pulses with centre wavelengths of 910 and 780 nm is analysed using a single-shot second-order intensity autocorrelator. It is shown that estimates of the single-cycle pulse duration with an error of less than 5% require the use of KDP crystals with a thickness of no more than 10 μm for the second harmonic generation. At the same time, to estimate the duration of a transform-limited pulse containing ten optical cycles, the crystal thickness can be up to 1 mm. In this case, at an optimum angle of convergence of the first-harmonic beams, the duration estimation error is less than 2%.**

Keywords: *autocorrelator, three-wave interaction, ultrashort laser pulses.*

1. Introduction

Modern oscilloscopes and photodiodes do not have a temporal resolution sufficient to directly measure the duration of femtosecond laser pulses. For this purpose, indirect methods and devices developed on their basis are used. Some of them allow one to measure the intensity correlation functions, while others use special algorithms to restore the temporal profile of the pulse and its spectral or temporal phase. The use of these or other methods is determined by the laser operation regime and characteristics of the pulses being diagnosed. Typically, to measure the temporal characteristics of single ultrashort pulses, the second-order [1–3] and third-order [4, 5] intensity autocorrelators are used, as well as single-shot FROG (frequency resolved optical gating), SPIDER (spectral phase interferometry for direct electric field reconstruction) [6] and GRENUILLE [7] devices. Single-shot second-order intensity correlators make it impossible to distinguish the leading and trailing edges of the pulse, while third-order intensity correlators make it possible. To diagnose laser pulses with a high repetition rate (tens of hertz and higher), scanning FROG and cross-correlators based on two-photon absorption [8] and second harmonic generation [9] are used. Due to the development of ultrahigh-power laser systems [10] that allow laser pulses to be generated with petawatt power and ultrashort duration (tens of femtoseconds or less), the task of correctly measuring the temporal characteristics of such radiation becomes urgent.

I.V. Kuzmin, S.Yu. Mironov, E.A. Khazanov Institute of Applied Physics, Russian Academy of Sciences, Russia, ul. Ulyanova 46, 603950 Nizhny Novgorod, Russia; e-mail: kuzminiv@appl.sci-nnov.ru

Received 4 March 2020
Kvantovaya Elektronika **50** (4) 354–360 (2020)
Translated by M.A. Monastyrskiy

Recently, methods of additional temporal compression of ultrahigh-power laser pulses have also been actively developed. One of them, called CAfCA (compression after compressor approach) [11], was successfully tested in experiments and allowed one to significantly reduce the radiation pulse duration [12–15]. As shown in work [16], the application of this method will allow further implementation of petawatt pulses with a single-cycle duration of light field oscillations in experiments. Diagnostics of the temporal parameters of such radiation is a nontrivial task, which, nonetheless, can be solved using the presently developed methods, with sufficient measurement accuracy being provided.

It is important to note that earlier single-shot intensity correlators of the second and third orders were used to diagnose ultrashort pulses. For the first time, the results of measurements of the duration of a femtosecond laser pulse using a single-shot second-order autocorrelator were presented in work [17]. The pulse duration was 50 fs, and the measurements were conducted using a 300-μm-thick KDP crystal. The possibility of autocorrelation measurements at pulse duration of ~100 fs with a dynamic range of 10^8 was shown in [18]. Using the dispersion scanning technique, Louisy et al. [19] demonstrated the possibility of obtaining the temporal envelope of a laser pulse with a duration of 4 fs in the single-shot regime. A single-shot cross-correlator with a dynamic range up to 10^{10}, subpicosecond resolution and a time window up to 70 ps was considered in [20, 21].

The ultrashort laser pulses obtained in experiments usually have a non-flat spectrum phase. When diagnosing ultrashort chirped pulses, the impact of the dispersion of the linear part of the nonlinear-crystal refractive index may lead to an incorrect evaluation of the autocorrelation function (ACF) width. In this case, the error can be evaluated using numerical methods. In the present work, we analyse the accuracy of the duration estimates of single-cycle laser pulses with centre wavelengths λ_0 = 910 and 780 nm by a single-shot second-order intensity autocorrelator. The simulation is performed for transform-limited pulses, as well as for pulses with quadratic and cubic modulation of the spectrum phase.

2. Optical scheme and principle of operation

Optical scheme of a single-shot second-order autocorrelator is shown in Fig. 1a. The laser pulse being measured is split into two replicas, which are directed to a nonlinear optical crystal where non-collinear generation of the second harmonic occurs (Fig. 1b). The non-collinear interaction scheme is necessary to implement the principle of converting the temporal intensity distribution into its spatial profile [17]. In this implementation, the transverse distribution of the second

harmonic radiation intensity in the near field at the nonlinear crystal output contains information about the temporal structure of the radiation being diagnosed. Optimal operation of the device assumes the detection of the second-order symmetric ACF intensity:

$$K(\tilde{\tau}) = \int_{-\infty}^{\infty} I_1(t-\tilde{\tau}) I_0(t)\,\mathrm{d}t, \qquad (1)$$

where $I_0(t)$ and $I_1(t-\tilde{\tau})$ are the temporal intensity distributions of the original pulse being diagnosed and the pulse that passed through the beam splitter. Ideally, their profiles are identical, i. e. $I_1(t) = I_0(t)$. However, as the duration of the diagnosed pulse tends to a single oscillation cycle in optical elements, the role of linear dispersion of the refractive index increases. There are two such elements in the device scheme: a beam splitter and a nonlinear crystal itself. Because of the dispersion in the beam splitter, the measured function ceases to correspond to the autocorrelation function. Its profile may not have symmetry, and the reconstructed information on the temporal pulse structure may be inaccurate.

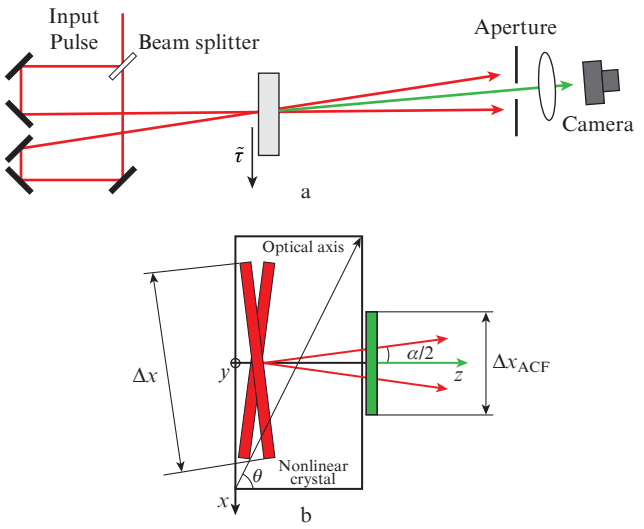

Figure 1. (a) Scheme for obtaining ACF under non-collinear second harmonic generation and (b) scheme of interaction of a pulse and its replica in a nonlinear crystal.

There are two ways to solve the beam splitter problem. The first method assumes splitting the beam without passing through the material medium. This can be achieved by reflecting part (for example, 50% of the area) of the beam with a mirror. Diffraction effects arising from this beam splitting can be eliminated by transferring the image by a spherical mirror onto the crystal surface. The second method is to compensate for the introduced material dispersion of the beam splitter by means of a chirped mirror installed in the path of the beam passing through the splitter. Obviously, the second approach is not optimal, since the chirped mirror cannot accurately compensate for the introduced dispersion of the second and higher orders. Moreover, the chirped mirror itself can additionally introduce an undesirable spectrum phase. Further we assume that the device implements a dispersion-free splitting of the laser beam. The effects of geometric factors and the refractive index dispersion of a nonlinear crystal on the interaction of pulses are considered in the following sections.

3. Effect of the interaction geometry of pulses on the accuracy of measurements of their duration

In this section, we neglect the effect of the refractive index dispersion of a nonlinear crystal on the second harmonic generation. Our aim is to determine the basic requirements for the interaction geometry of pulses that must be met for the correct measurement of the second-order ACF. Figure 1b shows a scheme of interaction of two pulses inside a nonlinear crystal. Since, as mentioned above, the second harmonic is generated with a low efficiency, the measured signal is a function of the form

$$K_1(x) = \int_{-\infty}^{\infty} I_0(t-\beta x + t_0) I_0(t+\beta x)\,\mathrm{d}t, \qquad (2)$$

where I_0 is the intensity of the first harmonic radiation; t_0 is the time delay between the first harmonic pulses; $\beta = \sin(\alpha/2)/v_z$; α is the angle between the directions of propagation of the first harmonic beams inside the crystal; v_z is the projection of the group velocity of the first harmonic pulse on the z axis; and x is the transverse coordinate (Fig. 1b). Expression (2) can be analytically integrated for pulses with a Gaussian intensity distribution:

$$I_0(x,y,t) = I_0 \exp\left(-4\frac{x^2+y^2}{\Delta x^2}\right)\exp\left(-4\ln 2\frac{t^2}{\Delta t^2}\right), \qquad (3)$$

where Δx is the full beam size at the 1/e level, and Δt is the FWHM pulse duration. The result of integration is a Gaussian function with a Δx_{ACF} width along the x axis at a 1/2 intensity level:

$$\frac{1}{\Delta x_{\mathrm{ACF}}^2} = \frac{2}{\ln 2 \Delta x^2} + \frac{2\beta^2}{\Delta t^2}. \qquad (4)$$

A time delay of one of the pulses by a value of t_0 shifts the ACF maximum by $\Delta x_0 = t_0\beta \times \Delta x_{\mathrm{ACF}}^2/\Delta t^2$. Since the principle of linear transformation of the temporal coordinate into the spatial one is implemented in the correlator under consideration, this relation, together with (4), allows us to find a relationship between the ACF width Δt_{ACF} and the duration Δt of the pulse being diagnosed:

$$\Delta t_{\mathrm{ACF}}^2 = 2\Delta t^2\left(1 + \frac{\Delta t^2}{\ln 2 \beta^2 \Delta x^2}\right). \qquad (5)$$

At the same time, the relationship between the ACF width and the pulse duration with a Gaussian intensity distribution is well known: $\Delta t_{\mathrm{ACF}}^2 = 2\Delta t^2$. A comparison of this relationship with formula (5) shows that the intensity autocorrelator always introduces a systematic error in determining the duration. Since the second term on the right-hand side of formula (5) is positive, this error leads to an overestimation of the pulse duration.

Within the framework of the approximation in question, increasing the beam diameter Δx and the angle α between the interacting first-harmonic pulses inside the nonlinear element reduces the error. In particular, for pulses with a duration of one, three, and ten field cycles ($\Delta t = p\lambda_0/c$, where $p = 1, 3, 10$, and $\lambda_0 = 910$ nm) with a beam diameter $\Delta x = 1$ mm and an angle $\alpha = 1°$, the error in determining the duration is 0.4%, 4% and 30%, respectively. To minimise this error in further

calculations, we assume that Δx is equal to 2 mm; in this case, for the specified durations, the error is 0.1%, 1% and 8%, respectively. Note that the geometric error can also be eliminated by introducing additional correction, but it is more efficient to use a relation between the beam size and the pulse duration at which the error is negligible.

4. Effect of linear dispersion of the refractive index of a nonlinear crystal on the duration evaluation accuracy

4.1. Equations and initial boundary conditions

In this section, we analyse the effect of linear dispersion of the refractive index of the crystal in which the second harmonic is generated on the accuracy of the duration estimates of ultrashort laser pulses. To this end, we obtain equations describing the process of non-collinear generation of the second harmonic by pulses with a duration equal to a single cycle of field oscillations. We use the slowly evolving wave approximation (SEWA) [22], which is more accurate than the slowly varying amplitude approximation (SVAA) [23]. To derive equations using this method, we use the approximation

$$\left|\frac{\partial E}{\partial z}\right| \ll k_0|E| \text{ or } |(k_0 - k_1\omega_0)/k_0| \ll 1,$$

which is valid for a wider range of parameters compared to the approximation $[k(\omega) + k_0]/(2k_0) \approx 1$ used in the SVAA method. Here, $k(\omega) = (\omega/c)\sqrt{\varepsilon(\omega)}$ is the dependence of the wavenumber on the frequency ω; $\varepsilon(\omega)$ is permittivity; k_0 is the wavenumber for the centre frequency ω_0; $E = \tilde{A}(t, r_\perp, z) \times \exp[\mathrm{i}(\omega_0 t - k_0 z + \psi] + \text{c.c.}$ is the electric field intensity of the light wave; k_1^{-1} is the group velocity of the laser pulse for the centre frequency; and $\tilde{A}(t, r_\perp, z)$ is the complex amplitude.

Within the framework of this approximation, the equation for the electric field amplitude in the accompanying coordinate system can be obtained directly from Maxwell's equations ($\tau = t - k_1 z$, $\partial_\tau \to \partial_t$, $\partial_z \to \partial_z - k_1\partial_\tau$) (see the Appendix):

$$\partial_z\tilde{A} + \mathrm{i}\hat{D}\tilde{A} - \frac{1}{2k_0}\left(\mathrm{i} + \frac{k_1}{k_0}\partial_\tau\right)^{-1}(\Delta_\perp + \hat{D}^2 + \partial_z^2)\tilde{A}$$

$$= -\frac{2\pi}{c^2}\frac{\omega_0^2}{k_0}\left(\mathrm{i} + \frac{1}{\omega_0}\partial_\tau\right)^2\left(\mathrm{i} + \frac{k_1}{k_0}\partial_\tau\right)^{-1}\tilde{P}, \qquad (6)$$

where

$$\hat{D} = \sum_{m=0}^{\infty}\frac{k_m}{m!}(-\mathrm{i}\partial_t)^m + \mathrm{i}k_1\partial_t - k_0$$

is the dispersion operator;

$$k_m = \left.\frac{\partial^m k(\omega)}{\partial\omega^m}\right|_{\omega=\omega_0};$$

and $\tilde{P}$ is the nonlinear polarisation amplitude. When deriving equation (6), absorption in the medium is neglected. As applied to the process of non-collinear second harmonic generation, from equation (6), with allowance for the additional condition $(k_1^2/k_0^2)\partial_\tau^2 \ll 1$, we can obtain a system of coupled equations in the paraxial approximation (see the Appendix):

$$\partial_z\hat{A}_1(\Omega, r_\perp, z) + \mathrm{i}\left[\hat{D}_{1\omega} + \left(1 - \frac{k_{31}}{k_{1z0}}\Omega\right)\frac{\Delta_\perp + \hat{D}_{1\omega}^2}{2k_{1z0}}\right]\hat{A}_1(\Omega, r_\perp, z)$$

$$= -\frac{2\pi}{c^2}\frac{\omega_{10}^2 d_{\text{eff}}}{k_{1z0}}\mathbb{F}\left\{\left[\mathrm{i} + \left(\frac{2}{\omega_{10}} - \frac{k_{31}}{k_{1z0}}\right)\partial_\tau\right]\tilde{A}_2^*(\tau, r_\perp, z)\right.$$

$$\left.\times\ \tilde{A}_3(\tau, r_\perp, z)\right\}\exp(\mathrm{i}\Delta k z),$$

$$\partial_z\hat{A}_2(\Omega, r_\perp, z) + \mathrm{i}\left[\hat{D}_{2\omega} + \left(1 - \frac{k_{31}}{k_{2z0}}\Omega\right)\frac{\Delta_\perp + \hat{D}_{2\omega}^2}{2k_{2z0}}\right]\hat{A}_2(\Omega, r_\perp, z)$$

$$= -\frac{2\pi}{c^2}\frac{\omega_{20}^2 d_{\text{eff}}}{k_{2z0}}\mathbb{F}\left\{\left[\mathrm{i} + \left(\frac{2}{\omega_{20}} - \frac{k_{31}}{k_{2z0}}\right)\partial_\tau\right]\tilde{A}_1^*(\tau, r_\perp, z)\right. \qquad (7)$$

$$\left.\times\ \tilde{A}_3(\tau, r_\perp, z)\right\}\exp(\mathrm{i}\Delta k z),$$

$$\partial_z\hat{A}_3(\Omega, r_\perp, z) + \mathrm{i}\left[\hat{D}_{3\omega} + \left(1 - \frac{k_{31}}{k_{3z0}}\Omega\right)\frac{\Delta_\perp + \hat{D}_{3\omega}^2}{2k_{3z0}} + (\tan\rho)\partial_y\right]$$

$$\times\hat{A}_3(\Omega, r_\perp, z) = -\frac{2\pi}{c^2}\frac{\omega_{30}^2 d_{\text{eff}}}{k_{3z0}}\mathbb{F}\left\{\left[\mathrm{i} + \left(\frac{2}{\omega_{30}} - \frac{k_{31}}{k_{3z0}}\right)\partial_\tau\right]\tilde{A}_1(\tau, r_\perp, z)\right.$$

$$\left.\times\ \tilde{A}_2(\tau, r_\perp, z)\right\}\exp(-\mathrm{i}\Delta k z).$$

Here $\hat{A}_j(\Omega, r_\perp, z)$ is the Fourier transform of the complex amplitudes $\tilde{A}_j(\tau, r_\perp, z)$ of interacting pulses; k_{jz0} and ω_{j0} are the projections of wave vectors onto the z axis and the centre frequencies of interacting pulses; $\hat{D}_{j\omega} = k_j(\omega) - v_3^{-1}\Omega - k_{jz0}$ is the dispersion factor; $v_3 = k_{31}^{-1}$ is the group velocity of radiation at the sum frequency; d_{eff} is the crystal nonlinearity coefficient; ρ is the walk-off angle; and $\Delta k = k_{1z0} + k_{2z0} - k_{3z0}$ is the wave detuning from the phase-matching direction at the centre frequency. The peculiarity of this system of equations is a more accurate accounting of dispersion effects, which allows us to describe the interaction of ultrashort optical pulses. When performing calculations, the dispersion relation relies on the exact Sellmeier equations in the studied spectral range instead of the series terms.

As boundary conditions, we consider pulsed beams with a quasi-plane transverse intensity distribution (the degree of the super-Gaussian function is 6) and Gaussian distribution in time. Note that the system of equations (7) allows us to use as boundary conditions pulsed beams with an arbitrary intensity distribution and an arbitrary spectrum phase (including those measured in experiments). To demonstrate the effect of chirp on the accuracy of measuring the duration of few-cycle pulses, a third-order spectrum phase expansion was used. It is convenient to set initial conditions for the spectral components of the field at the crystal input boundary:

$$\hat{A}_1(\Omega, x, y) = A_{01}\exp\left(-\frac{x^6}{2\Delta x^6} - \frac{y^6}{2\Delta y^6}\right)$$

$$\times\exp\left(-\mathrm{i}\Omega x\frac{\tan(\alpha/2)}{v_z}\right)\exp\left(-\frac{2\ln 2\,\Omega^2}{\Delta\Omega^2}\right)$$

$$\times\exp\left(-\mathrm{i}\varphi_1\frac{\Omega^2}{2} - \mathrm{i}\varphi_2\frac{\Omega^3}{6}\right), \qquad (8)$$

$$\hat{A}_2(\Omega, x, y) = A_{02}\exp\left(-\frac{x^6}{2\Delta x^6} - \frac{y^6}{2\Delta y^6}\right)$$

$$\times \exp\left(\mathrm{i}\Omega x \frac{\tan(\alpha/2)}{v_z}\right)\exp\left(-\frac{2\ln 2\,\Omega^2}{\Delta\Omega^2}\right)$$

$$\times \exp\left(-\mathrm{i}\varphi_1\frac{\Omega^2}{2}-\mathrm{i}\varphi_2\frac{\Omega^3}{6}\right), \qquad (9)$$

where $\Omega = \omega_0 - \omega$ is the centre frequency detuning; $\Delta\Omega$ is the full spectrum width at the 1/2 intensity level; and φ_1 and φ_2 are the parameters of quadratic and cubic phase modulation. Initial conditions (8) and (9) take into account the fact that ultrashort pulses acquire an angular chirp and the corresponding slope of the amplitude front as a result of refraction at the crystal boundary. The system of equations (7) together with initial boundary conditions (8) and (9) can be used to simulate a single-shot second-order intensity autocorrelator applied for measuring the duration of few-cycle (up to a cycle of optical oscillations) pulses. In this system of equations, the initial phase of field oscillations does not affect the resulting ACF regardless of the pulse duration.

4.2. Numerical simulation of a single-shot autocorrelator

Let us analyse the accuracy of estimating the duration of laser pulses using an intensity autocorrelator. We consider radiation with centre wavelengths $\lambda_0 = 910$ nm (OPCPA system on DKDP crystals) and 780 nm (laser complexes with Ti:sapphire amplifiers) and pulse durations of one, three, and ten field cycles corresponding to 3, 9 and 30 fs (2.6, 7.8 and 26 fs) for pulses with $\lambda_0 = 910$ nm (780 nm). It is assumed that, in the cross-correlator crystal, the laser beams intersect in a plane that makes the phase matching noncritical. As a nonlinear element used for the second harmonic generation, KDP crystals with a thickness of 10–1000 μm are considered. The beam diameter Δx is chosen equal to 2 mm to minimise the contribution of the geometric error in accordance with Section 3. The KDP crystal is used in the second-order intensity autocorrelator that serves to diagnose the temporal characteristics of radiation at the output of a PEARL subpetawatt laser complex ($\lambda_0 = 910$ nm). The choice of this type of crystal is due to the fact that, in the specified spectral region, it has rather weak dispersion in the linear part of the refractive index: $k_{12} = 11$ fs^2 mm^{-1} and $k_{22} = 82$ fs^2 mm^{-1} for the first and second harmonics, respectively. The group dispersion of the pulses of the first and second harmonics is $\Delta v = 36$ fs mm^{-1}. At the same time, for radiation from Ti:sapphire lasers with $\lambda_0 \approx$ 780 nm, the KDP crystal has significantly greater dispersion ($k_{12} = 30$ fs^2 mm^{-1}, $k_{22} = 103$ fs^2 mm^{-1}, $\Delta v = 77$ fs mm^{-1}) which affects the accuracy of the duration estimates.

The system of coupled equations (7) was solved using the split-step Fourier method [23]. The dependences of the ratio of the 'measured' pulse duration $\tau_m = \Delta t_{ACF}/\sqrt{2}$ to the initial pulse duration τ_0 on the convergence angle and the crystal thickness are shown in Figs 2 and 3 for radiation with $\lambda_0 =$ 910 and 780 nm. The simulation was performed for transform-limited pulses ($\varphi_1 = 0$, $\varphi_2 = 0$).

The dependences shown in Fig. 2 have a unique extremum corresponding to the optimum convergence angle α between the first-harmonic pulses inside the crystal. The extremum is caused, on the one hand, by the ACF broadening at small α [see expression (5)], and, on the other hand, by the dispersion broadening of interacting pulses in the crystal. When diagnosing laser pulses with $\lambda_0 = 780$ nm, the contribution of dispersion effects to the measurement result becomes more significant than that for the duration of pulses with $\lambda_0 = 910$ nm.

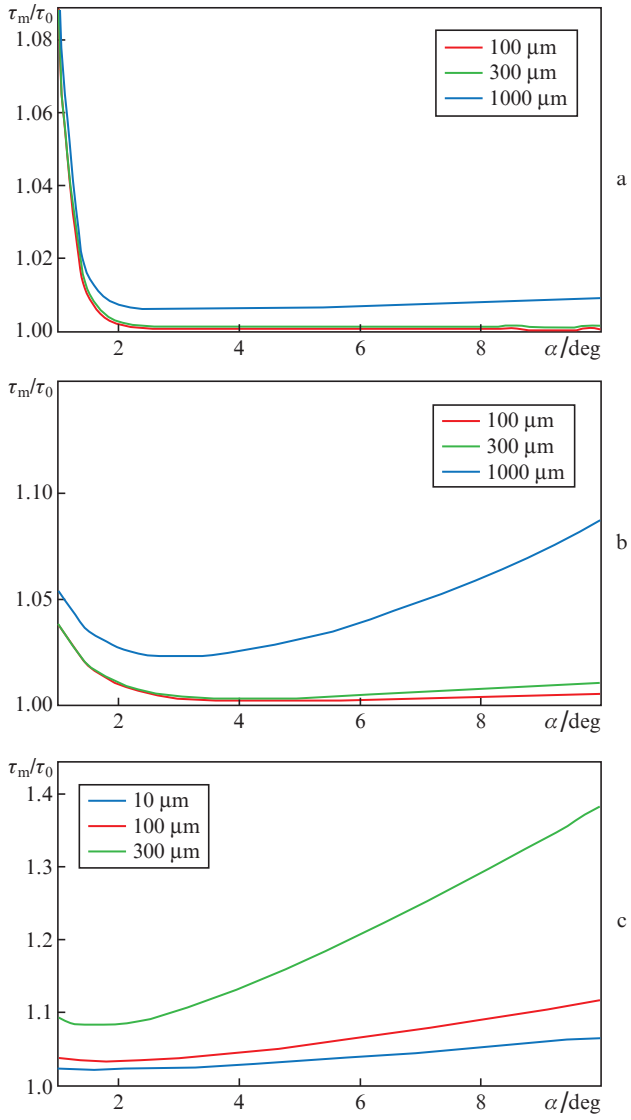

Figure 2. (Colour online) Dependences of the ratio τ_m/τ_0 on the convergence angle α for pulses with a duration of (a) ten field cycles, (b) three cycles and (c) one cycle for various crystal thicknesses and $\lambda_0 =$ 910 nm.

The duration measurement accuracy is reduced. For pulses with a duration of ten optical cycles and more, we have observed no significant differences in the duration estimates.

Consider the effect of quadratic phase modulation on the accuracy of pulse duration evaluation ($\varphi_1 \neq 0, \varphi_2 = 0$). Figure 4a shows the dependence of the ratio τ_m/τ_0 on the convergence angle α and the crystal thickness. The spectral width of the laser pulse corresponds to the duration of one cycle of field oscillations (wavelength 780 nm), while the duration is increased to about four oscillations.

Figure 4b demonstrates the effect of cubic phase modulation on the accuracy of the ACF width evaluation ($\varphi_1 = 0$, $\varphi_2 \neq 0$). It can be seen that when the crystal thickness exceeds 10 μm, the measured function for the pulses under consideration differs significantly from the ACF, which leads to erroneous results in measuring the duration. We also note that the sign of phase modulation also affects the measurement results. Thus, when measuring the duration of ultra-wideband laser pulses, which generally have phase

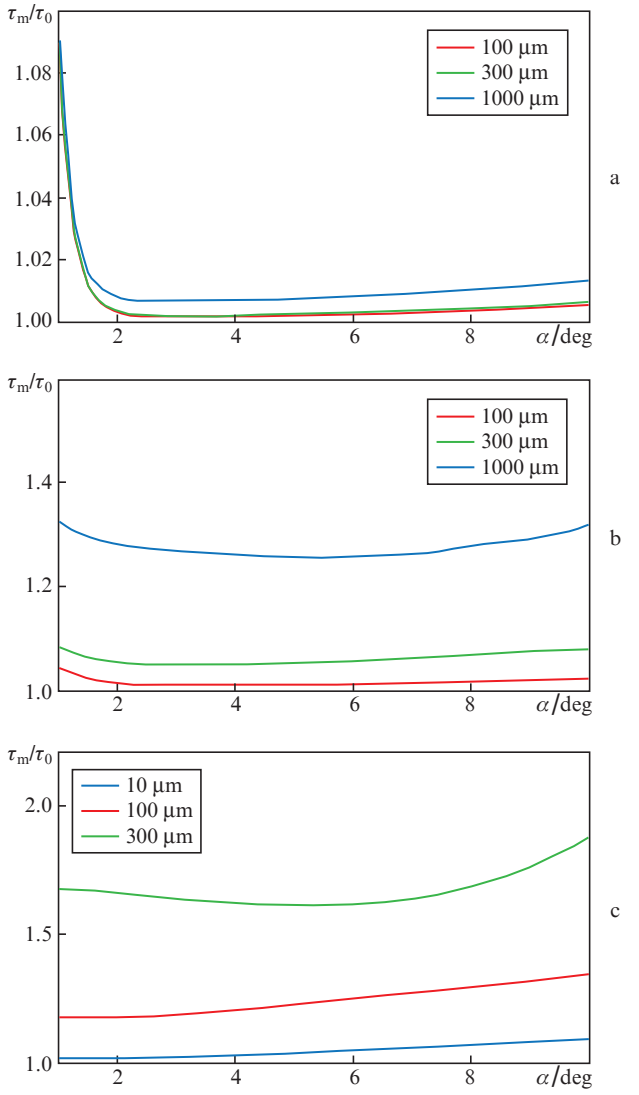

Figure 3. (Colour online) Dependences of the ratio τ_m/τ_0 on the convergence angle α for pulses with a duration of (a) ten field cycles, (b) three cycles and (c) one cycle for various crystal thicknesses and λ_0 = 780 nm.

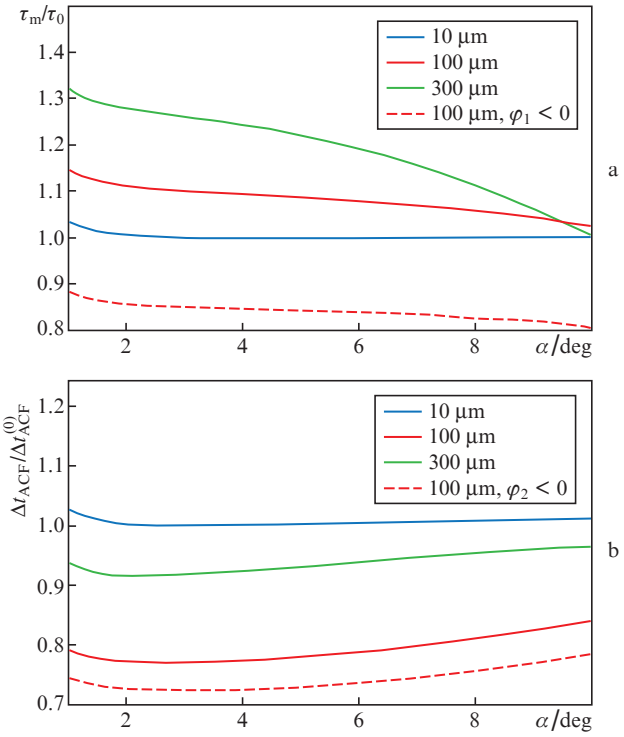

Figure 4. (Colour online) Dependences of (a) the ratio τ_m/τ_0 for a linearly chirped pulse with a duration of about four field cycles and (b) the ratio of the 'measured' ACF width to the original one ($\Delta t_{ACF}/\Delta t_{ACF}^{(0)}$) for a pulse with cubic phase modulation on the convergence angle α at different crystal thicknesses and λ_0 = 780 nm.

modulation of various orders, the KDP crystal thickness should not exceed 10 μm, which ensures the duration evaluation accuracy better than 5%.

At the same time, a crystal with a thickness of up to 1 mm can be used to estimate the duration of transform-limited pulses of about ten optical cycles. In this case, at the optimum convergence angle of the first-harmonic beams, the duration evaluation accuracy is better than 1% and even at the non-optimal angle is 2% (see Fig. 2a).

5. Conclusions

We have analysed the possibility of using a single-shot intensity autocorrelator to evaluate the duration of single-cycle laser pulses with centre wavelengths of 910 and 780 nm. It is shown that the accuracy of the restored duration for transform-limited pulses depends both on the nonlinear crystal thickness and the convergence angle of the first harmonic beams. However, there is an optimal angle at which the duration is restored with the least error. When diagnosing ultra-wide-band laser pulses, it is necessary to use KDP crystals with a thickness of no more than 10 μm, which ensures that the accuracy of the pulse duration evaluation is no worse than 5%. Nevertheless, to evaluate the pulse duration of about ten optical cycles, the crystal thickness can be chosen equal to 1 mm. In this case, with the optimum convergence angle, the accuracy of the pulse duration evaluation is better than 2%.

Acknowledgements. This work was supported by the Ministry of Science and Higher Education of the Russian Federation (No. 0030-2020-0022).

Appendix. Derivation of the equations used and validity evaluation of the corresponding approximations

The original nonlinear wave equation for the electric field appears as:

$$(\partial_z^2 + \Delta_\perp)E(\boldsymbol{r},t) - \frac{1}{c^2}\partial_t^2 \int_{-\infty}^{t} \varepsilon(t-t')E(\boldsymbol{r},t')\,\mathrm{d}t' = \frac{4\pi}{c^2}\partial_t^2 P_{\mathrm{nl}}(\boldsymbol{r},t). \quad \text{(A1)}$$

Let us represent the fields through their envelopes:

$$E(\boldsymbol{r},t) = \tilde{A}(t,\boldsymbol{r}_\perp,z)\exp[\mathrm{i}(\omega_0 t - k_0 z + \psi)],$$
$$P_{\mathrm{nl}}(\boldsymbol{r},t) = \tilde{P}(\boldsymbol{r}_\perp,z,t)\exp[\mathrm{i}(\omega_0 t - k_0 z + \psi)]. \quad \text{(A2)}$$

Substituting (A2) into the wave equation we obtain the expression

$$(-k_0^2 - 2ik_0\partial_z + \partial_z^2 + \Delta_\perp)\tilde{A} + (k_0 - ik_1\partial_t + \hat{D})^2\tilde{A} = \frac{4\pi}{c^2}\omega_0^2\left(1 + \frac{1}{\omega_0}\partial_t\right)^2\tilde{P}. \quad \text{(A3)}$$

Here,

$$\hat{D} = \sum_{m=0}^{\infty}\frac{k_m}{m!}(-i\partial_t)^m + ik_1\partial_t - k_0$$

is the dispersion operator;

$$k_m = \left.\frac{\partial^m k(\omega)}{\partial\omega^m}\right|_{\omega=\omega_0};$$

and $k(\omega) = (\omega/c)\sqrt{\varepsilon(\omega)}$ is the dependence of the wavenumber on frequency. A similar equation was obtained in [22]. Next, we pass over to the accompanying coordinate system ($\tau = t - k_1 z$, $\partial_\tau \to \partial_t$, $\partial_z \to \partial_z - k_1\partial_\tau$) and rewrite equation (A3) in the form

$$[-k_0^2 - 2ik_0(\partial_z - k_1\partial_\tau) + (\partial_z - k_1\partial_\tau)^2 + \Delta_\perp]\tilde{A} + [k_0^2 + 2k_0(-ik_1\partial_\tau + \hat{D}) + (-ik_1\partial_\tau + \hat{D})^2]\tilde{A} = \frac{4\pi}{c^2}\omega_0^2\left(1 + \frac{1}{\omega_0}\partial_\tau\right)^2\tilde{P}. \quad \text{(A4)}$$

Let us open the brackets:

$$(-k_0^2 - 2ik_0\partial_z + 2ik_0k_1\partial_\tau + \partial_z^2 - 2k_1\partial_\tau\partial_z + k_1^2\partial_\tau^2 + \Delta_\perp)\tilde{A} + (k_0^2 - 2ik_0k_1\partial_\tau + 2k_0\hat{D} - k_1^2\partial_\tau^2 - 2ik_1\hat{D}\partial_\tau + \hat{D}^2)\tilde{A} = \frac{4\pi}{c^2}\omega_0^2\left(1 + \frac{1}{\omega_0}\partial_\tau\right)^2\tilde{P}, \quad \text{(A5)}$$

reduce similar terms with different signs:

$$(-2ik_0\partial_z + \partial_z^2 - 2k_1\partial_\tau\partial_z + \Delta_\perp)\tilde{A} + (2k_0\hat{D} - 2ik_1\hat{D}\partial_\tau + \hat{D}^2)\tilde{A} = \frac{4\pi}{c^2}\omega_0^2\left(1 + \frac{1}{\omega_0}\partial_\tau\right)^2\tilde{P}, \quad \text{(A6)}$$

and factor out the term $[1 + (k_1/k_0)\partial_t]$ on the left-hand side of equation (A6):

$$-2ik_0\left[(-i\partial_z + \hat{D})\left(i + \frac{k_1}{k_0}\partial_\tau\right) - \frac{\partial_z^2}{2ik_0} - \frac{\Delta_\perp}{2ik_0} - \frac{\hat{D}^2}{2ik_0}\right]\tilde{A} = \frac{4\pi}{c^2}\omega_0^2\left(1 + \frac{1}{\omega_0}\partial_\tau\right)^2\tilde{P}. \quad \text{(A7)}$$

Thus, we obtain

$$\partial_z\tilde{A} + i\hat{D}\tilde{A} - \frac{1}{2k_0}\left(1 + \frac{k_1}{k_0}\partial_\tau\right)^{-1}(\Delta_\perp\tilde{A} + \hat{D}^2\tilde{A} + \partial_z^2\tilde{A}) = -\frac{2\pi}{c^2}\frac{\omega_0^2}{k_0}\left(1 + \frac{1}{\omega_0}\partial_\tau\right)^2\left(1 + \frac{k_1}{k_0}\partial_\tau\right)^{-1}\tilde{P}. \quad \text{(A8)}$$

For further simplification, we take into account that

$$\frac{1}{1 + (k_1/k_0)\partial_\tau}\frac{-1 + (k_1/k_0)\partial_\tau}{-1 + (k_1/k_0)\partial_\tau} = \frac{-1 + (k_1/k_0)\partial_\tau}{1 + (k_1^2/k_0^2)\partial_\tau^2} \approx -1 + \frac{k_1}{k_0}\partial_\tau. \quad \text{(A9)}$$

After transformation, equation (A8) acquires the form:

$$\partial_z\tilde{A} + i\hat{D}\tilde{A} + \frac{1}{2k_0}\left(1 - \frac{k_1}{k_0}\partial_\tau\right)(\Delta_\perp\tilde{A} + \hat{D}^2\tilde{A} + \partial_z^2\tilde{A}) = \frac{2\pi}{c^2}\frac{\omega_0^2}{k_0}\left(1 + \frac{1}{\omega_0}\partial_\tau\right)^2\left(1 - \frac{k_1}{k_0}\partial_\tau\right)\tilde{P}. \quad \text{(A10)}$$

In the spectral region, the equation in the paraxial approximation reads as:

$$\partial_z\hat{A}(\Omega, r_\perp, z) + i\left[\hat{D}_\omega + \left(1 - \frac{k_1}{k_0}\Omega\right)\frac{\Delta_\perp + \hat{D}_\omega^2}{2k_0}\right]\hat{A}(\Omega, r_\perp, z) = \frac{2\pi}{c^2}\frac{\omega_0^2}{k_0}\mathbb{F}\left[\left(1 + \frac{1}{\omega_0}\partial_\tau\right)^2\left(1 - \frac{k_1}{k_0}\partial_\tau\right)\tilde{P}\right]. \quad \text{(A11)}$$

Here, $\mathbb{F}$ is the direct Fourier transform; $\hat{A}(\Omega, r_\perp, z)$ is the Fourier transform of the field amplitude $\tilde{A}(t, r_\perp, z)$; and

$$\hat{D}_\omega = \sum_{m=0}^{\infty}\frac{k_m}{m!}\Omega^m - k_1\Omega - k_0$$

is the dispersion factor. Equations (A10), (A11) can be used to describe nonlinear optical phenomena in the propagation of laser pulses, the duration of which is close to one optical cycle. In addition to the approximations used in [22], approximation (A9) must be satisfied. For non-collinear three-wave interaction, the dispersion operator $\hat{D}_\omega$ in the accompanying coordinate system has the form

$$\hat{D}_{j\omega} = \sum_{m=0}^{\infty}\frac{k_{jm}}{m!}\Omega^m - \frac{1}{v}\Omega - k_{jz0}. \quad \text{(A12)}$$

Here $j = 1-3$ are the indices of interacting laser pulses; k_{jz0} are the projections of wave vectors of interacting pulses at the centre frequency onto the z axis; and v is the group velocity along the z axis, which determines the direction of radiation propagation at a sum frequency.

In view of the foregoing, we obtain a system of equations describing the non-collinear generation of the third harmonic. We can present each of the interacting fields in the form:

$$\begin{aligned}
E_1(\boldsymbol{r}, t) &= \tilde{A}_1(t, \boldsymbol{r}_\perp, z)\exp[i(\omega_{10}t - k_{1z0}z + k_{1x0}x)],\\
P_1(\boldsymbol{r}, t) &= d_{\text{eff}}\tilde{A}_2^*\tilde{A}_3\exp\{i[(\omega_{30} - \omega_{20})t - (k_{3z0} - k_{2z0})z + k_{2x0}x]\},\\
E_2(\boldsymbol{r}, t) &= \tilde{A}_2(t, \boldsymbol{r}_\perp, z)\exp[i(\omega_{20}t - k_{2z0}z - k_{2x0}x)],\\
P_2(\boldsymbol{r}, t) &= d_{\text{eff}}\tilde{A}_1^*\tilde{A}_3\exp\{i[(\omega_{30} - \omega_{10})t - (k_{3z0} - k_{1z0})z - k_{1x0}x]\},\\
E_3(\boldsymbol{r}, t) &= \tilde{A}_3(t, \boldsymbol{r}_\perp, z)\exp[i(\omega_{30}t - k_{3z0}z)],
\end{aligned} \quad \text{(A13)}$$

$$P_3(\mathbf{r}, t) = d_{\text{eff}} \tilde{A}_1 \tilde{A}_2 \exp\{\mathrm{i}[(\omega_{10} + \omega_{20})t - (k_{1z0} - k_{2z0})z]\},$$

where k_{1x0} and k_{2x0} are the projections of wave vectors of interacting pulses at the centre frequency onto the x axis. Taking into account the nonlinear term in (A11) with the first derivative in time inclusive, we arrive at a system of equations that coincides with (7). This system of equations makes allowance for dispersion, diffraction (in the paraxial approximation), and beam walk-off, and thus can be used to describe the three-wave interaction of pulses with a duration of up to one optical cycle. We used it to describe the non-collinear generation of the second harmonic. It is worth noting that accounting for nonstationarity in the nonlinear term leads to the appearance of additional wave detuning, which depends on the duration of the interacting pulses and intensity. Equations (7) satisfy the SEWA approximation:

$$\left|\frac{k_0 - k_1\omega_0}{k_0}\right| \ll 1. \qquad \text{(A14)}$$

We should note that for radiation with a centre wavelength of 910 nm and characteristic time scale of 2 fs, the approximation $(k_1^2/k_0^2)\partial_\tau^2 \approx 0.06 \ll 1$ is satisfied. This approximation means that the characteristic scale of the field envelope change should be comparable to the cycle of oscillations. The non-collinearity between the interacting pulses ($\alpha \leqslant 10^\circ$) in three-wave interaction allows the use of the paraxial approximation ($k_{1x0}/k_{1z0} = \tan(\alpha/2) = \tan 5^\circ \approx 0.09 \ll 1$).

References

1. Janszky J., Corradi G., Gyuzalian R.N. *Opt. Commun.*, **23**, 293 (1977).
2. Raghuramaiah M., Sharma A.K., Naik P.A., Gupta P.D., Ganeev R.A. *Sadhana*, **26**, 603 (2001).
3. Ishida Y., Yajima T., Watanabe A. *Opt. Commun.*, **56**, 57 (1985).
4. Collier J., Hernandez-Gomez C., Allott R., Danson C., Hall A. *Laser Part. Beams*, **19**, 231 (2001).
5. Ginzburg V.N., Didenko N.V., Konyashchenko A.V., Lozhkarev V.V., Luchinin G.A., Lutsenko A., Mironov S.Yu., Khazanov E.A., Yakovlev I.V. *Quantum Electron.*, **38**, 1027 (2008) [*Kvantovaya Elektron.*, **38**, 1027 (2008)].
6. French D., Dorrer C., Jovanovic I. *Opt. Lett.*, **34**, 3415 (2009).
7. Akturk S., Kimmel M., O'Shea P., Trebino R. *Opt. Express*, **11**, 68 (2003).
8. Chen C., Rifani M., Cha J., Yin Y.-Y., Elliott D.S. *Phys. Rev. A*, **49**, 461 (1994).
9. Zelenogorskii V.V., Andrianov A.V., Gacheva E.I., Gelikov G.V., Krasilnikov M., Mart'yanov M.A., Mironov S.Yu., Potemkin A.K., Syresin E.M., Stephan F., Khazanov E.A. *Quantum Electron.*, **44**, 76 (2014) [*Kvantovaya Elektron.*, **44**, 76 (2014)].
10. Zeng X., Zhou K., Zuo Y., Zhu Q., Su J., Wang X., Jing F. *Opt. Lett.*, **42**, 2014 (2017).
11. Khazanov E.A., Mironov S.Yu., Mourou G. *Phys. Usp.*, **62**, 1096 (2019) [*Usp. Fiz. Nauk*, **189**, 1173 (2019)].
12. Mironov S., Lassonde P., Kieffer J.C., Khazanov E., Mourou G. *Eur. Phys. J. Spec. Top.*, **223**, 1175 (2014).
13. Lassonde P., Mironov S., Fourmaux S., Payeur S., Khazanov E., Sergeev A., Kieffer J.C., Mourou G. *Laser Phys. Lett.*, **13**, 075401 (2016).
14. Mironov S.Yu., Ginzburg V.N., Yakovlev I.V., Kochetkov A.A., Shaykin A.A., Khazanov E.A., Mourou G.A. *Quantum Electron.*, **47**, 614 (2017) [*Kvantovaya Elektron.*, **47**, 614 (2017)].
15. Ginzburg V.N., Yakovlev I.V., Zuev A.S., Korobeynikova A.P., Kochetkov A.A., Kuz'min A.A., Mironov S.Yu., Shaykin A.A., Shaikin I.A., Khazanov E.A. *Quantum Electron.*, **49**, 299 (2019) [*Kvantovaya Elektron.*, **49**, 299 (2019)].
16. Mourou G., Mironov S., Khazanov E., Sergeev A. *Eur. Phys. J. Spec. Top.*, **223**, 1181 (2014).
17. Salin F., Georges P., Roger G., Brun A. *Appl. Opt.*, **26**, 4528 (1987).
18. Braun A., Jung I.D., Rudd J.V., Cheng H., Weingarten K.J., Mourou G., Keller U. *Opt. Lett.*, **20**, 1889 (1995).
19. Louisy M., Guo C., Neoričič L., Zhong S., L'Huillier A., Arnold C.L., Miranda M. *Appl. Opt.*, **56**, 9084 (2017).
20. Ma J., Yuan P., Wang J., Xie G., Zhu H., Qian L. *High Power Laser Sci. Eng.*, **6**, e61 (2018).
21. Wang Y., Ma J., Wang J., Yuan P., Xie G., Ge X., Qian L. *Sci. Rep.*, **4**, 3818 (2014).
22. Brabec T., Krausz F. *Phys. Rev. Lett.*, **78**, 3282 (1997).
23. Agrawal G.P. *Nonlinear Fiber Optics* (New York: Acad. Press, 1995).